Progress in Simulation of Vortex-Induced Vibration

Hugh Blackburn
CSIRO Division of Building, Construction and Engineering

Ron Henderson
California Institute of Technology

1 Introduction

This paper describes and discusses recent digital computer simulations of vortex-induced vibration of circular cylinders. One of the major problems in producing simplified models of vortex-induced oscillations of lightly-damped slender structures is just that the physics of the flows are as yet poorly documented and understood. In the last decade, for example, a number of significant new features of bluff-body wakes have been found by experimentalists, and these results must eventually be reconciled with engineering models for prediction of vortex-induced vibrations. Computer simulations can ease the observational difficulties in these flows and aid in understanding the physics of vortex-induced vibration.

Results for fixed cylinders and cylinders in forced and vortex-induced oscillations will be presented for two- and three-dimensional calculations in the Reynolds number range 200–500.

2 Method

In the simulations to be described here, the Navier–Stokes equations have been solved in an accelerating frame of reference attached to the cylinder. This means that the computational mesh does not have to distort to accommodate cylinder motion, as in some other methods, but a forcing term has to be added to the Navier–Stokes equations in order to account for the acceleration of the reference frame, and the boundary conditions also have to be adjusted appropriately at each timestep. If the cylinder is in forced oscillation, the frame accelerations and velocities are known functions of time, however in the case of vortex-induced oscillation, the cylinder moves in under the influence of pressure and viscous forces applied by the fluid and structural stiffness and damping forces, so a set of body-motion ODEs are coupled to the Navier–Stokes and continuity equations.

This method is implemented directly for two-dimensional simulations, using a finite element technique with spectral accuracy for the spatial discretization, and a high-order time-splitting scheme for temporal integration. For three-dimensional simulations, the flow is assumed to be periodic along the cylinder span, allowing a Fourier decomposition in the spanwise direction, in which case a set of equations directly analogous to the 2D Navier–Stokes equations must be solved for each Fourier mode. Each mode can then be integrated forward in time, in parallel on independent processors, with inter-processor communication required only during formation of the nonlinear terms in the Navier–Stokes equations. Since the zeroth Fourier mode describes spanwise-mean flows and forces, only one processor needs to implement frame-motion inertial terms, time-varying boundary conditions, and integration of the ODEs. For more detailed discussions of the numerical technique, see Blackburn & Karniadakis (1993), Blackburn & Henderson (1994).

In order to reduce problems associated with cross-flow blockage and finite inflow and outflow lengths to a minimum, the computational domain was chosen to be at least 25 cylinder diameters

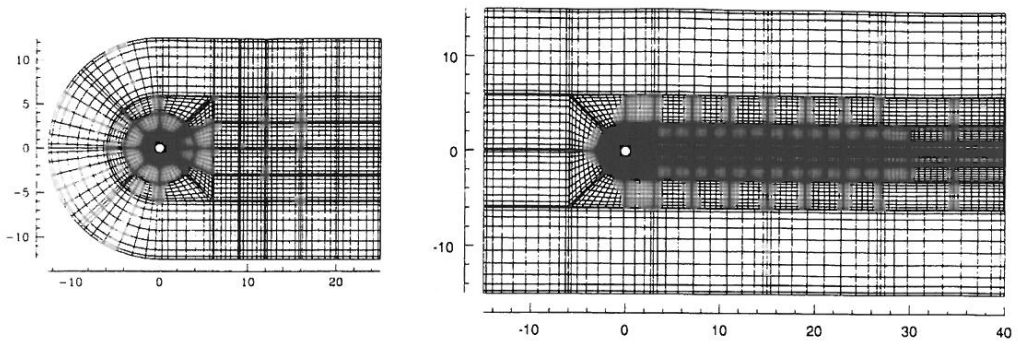

Figure 1: Gauss–Lobatto–Legendre finite element meshes used for $Re \leq 250$ (left) and $Re = 500$ (right).

across and 25 diameters long downstream of the cylinder. In the Reynolds number range of the simulations, the cross-flow dimension may be reduced as Re increases, however it has been found that the size of the domain has to be increased substantially in the streamwise direction with increasing Re to maintain numerical stability, particularly when the cylinder has substantial cross-flow oscillation amplitude; at $Re = 500$, the outflow distance required is of the order of 40 diameters. As Reynolds numbers rise, the spatial resolution must also be increased, with a consequent reduction in timestep demanded by the CFL stability criterion. In order to balance the requirements of fine spatial resolution, large domain size, while at the same time minimizing computer memory requirements, a mesh patching scheme has been introduced for non-conforming meshes (Henderson & Karniadakis 1993). The conforming mesh used for simulations at $Re \leq 250$ and the non-conforming mesh used at $Re = 500$ are shown in figure 1.

3 Results

Figure 2 shows results from two-dimensional forced-oscillation simulations carried out at $Re = 200$; a range of cylinder oscillation frequencies were employed at three cross-flow oscillation amplitudes: $\pm 0.1\,D$, $\pm 0.2\,D$ and $\pm 0,5\,D$, where D is the cylinder diameter. The shaded band on the figure shows the approximate limits of lock-in, where the vortex shedding frequency was the same as that of the forced oscillation. The now-familiar shape (the "A'rnold tongue" of chaos theory) is seen to emerge, in agreement with experimental results obtained at similar and higher Reynolds numbers.

At the same value of Reynolds number, vortex-induced vibrations were simulated and a range of oscillation amplitudes were obtained by varying the cylinder damping ratio ζ and the density ratio $m/\rho D^2$, which are often combined in the mass-damping parameter $m\zeta/\rho D^2$ (i.e. the Scruton number divided by 4π). Here it is a comparatively simple matter to study the effects of varying the two parts of the mass-damping parameter separately, and the results are shown in figure 3, plotted against a compilation of experimental results (Griffin 1992). A number of features may be noted: firstly, the overall shape of the experimental results is reproduced; secondly, limiting amplitudes in the limit $\zeta \to 0$ are observed in both the experimental and computational results; the lack of agreement in amplitude between experiments and simulations might be attributed to the wide disparity in Reynolds numbers (computations: 200; experiments: 300–10^6). Thirdly, the combination of the density and damping ratios into a single parameter is not quite valid in the low-damping limit (associated with the fact that the motions are not simple harmonic). Finally, the cross-flow oscillation amplitudes are overpredicted at high values of $m\zeta/\rho D^2$ (which are typical for wind engineering applications); this is most likely

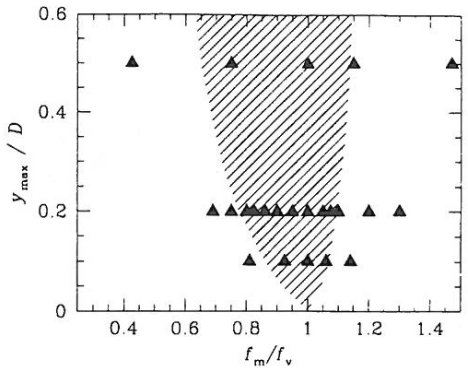

Figure 2: Frequency-amplitude envelope employed for forced-oscillation computations at $Re = 200$. Approximate limits within which lock-in was observed are shown shaded.

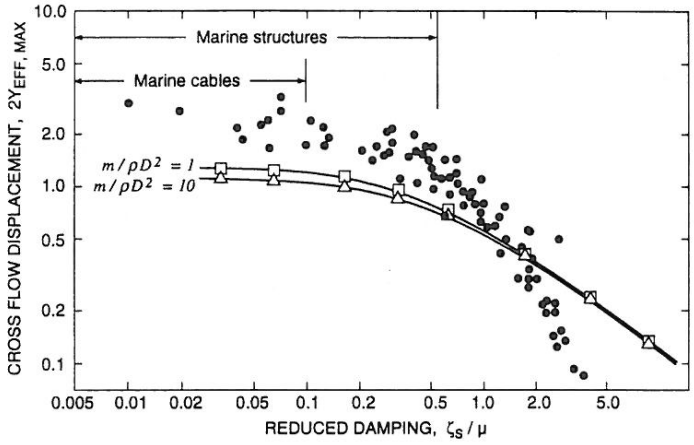

Figure 3: Maximum values of steady-state peak-to-peak free vibration oscillation amplitudes at $Re = 200$ as functions of the mass-damping product $\zeta_s/\mu = 8\pi^2 St^2 m\zeta/\rho D^2$. A comparison of computed values for density ratios $m/\rho D^2 = 1$ and 10 with a compilation of experimental values reproduced from Griffin (1992).

a consequence of the inability of the two-dimensional simulations to reproduce the significant three-dimensionality and consequent loss of spanwise coherence of lift forces found in flows at higher Reynolds numbers.

A significant feature of cylinder wakes reported from experiments employing forced cross-flow oscillations at $Re < 1\,000$ by Williamson & Roshko (1988) is the presence of regimes of amplitude and frequency in which the "classical" vortex-street wake behaviour is modified so that *two* pairs of vortices are shed per cycle of cylinder motion (the "2P" mode). In addition, an asymmetric regime was found, with a pair of vortices on one side of the wake, and a single vortex on the other (the "P+S" mode). In the 2D simulations reported in Blackburn & Henderson (1994), only the conventional "2S" mode was observed, and it was conjectured that the at the lower Reynolds numbers employed there ($Re = 250$), the other wake modes were not observed as a consequence of the increased diffusivity of vorticity at Reynolds numbers lower than those employed by Williamson & Roshko. We show in figure 4 results for a 2D simulation carried out at $Re = 500$ with the non-conforming mesh of figure 1 and a forced cross-flow oscillation

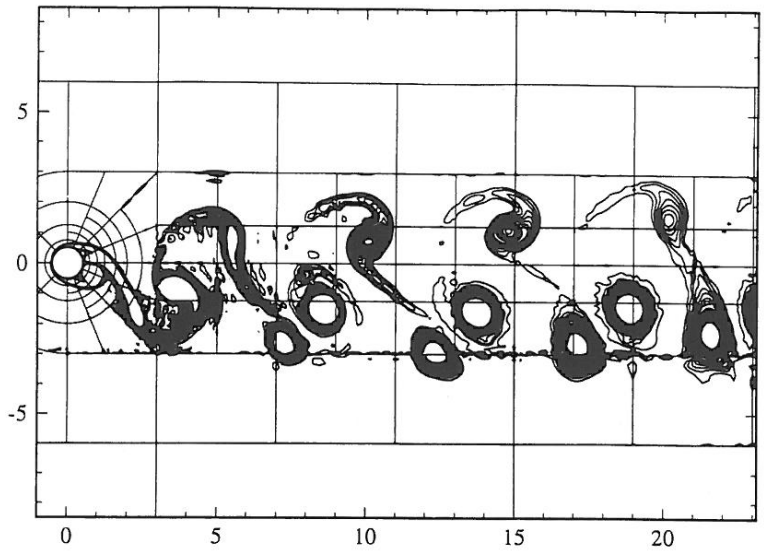

Figure 4: Vorticity contours for a 2D simulation at $Re = 500$ with forced cross-flow oscillation amplitude of $\pm 0.5\,D$, showing the "P+S" mode observed in the experiments of Williamson & Roshko (1988).

amplitude of $\pm 0.5\,D$: the "P+S" vortex-shedding mode is clearly visible.

4 Discussion and Conclusion

While computer simulations can not as yet successfully deal with the wide range of Reynolds numbers found in typical engineering applications, many of the basic physical processes can be found in the range of Reynolds numbers that can currently simulated directly: full simulations of three-dimensional cylinder wake flows can at present reach Reynolds numbers of around 1 000 and with some development of large eddy simulation techniques, much larger Reynolds numbers will soon be attempted. The results presented here should indicate the possibilities of application of computer simulation techniques to fundamental problems of vortex-induced vibration.

5 References

BLACKBURN, H. M. & HENDERSON, R. D. 1994. Lock-in behaviour in simulated vortex-induced vibration. Submitted to *Exptl Thermal & Fluid Sci.*.

BLACKBURN, H. M. & KARNIADAKIS, G. E. 1993. Two- and three-dimensional simulations of vortex-induced vibration of a circular cylinder. In *Proc. 3rd Int. Offshore & Polar Engng Conf.*, Singapore, Vol. 3, 715–720.

GRIFFIN, O. M. 1992. Vortex-induced vibrations of marine structures in uniform and sheared currents, *NSF Workshop on Riser Dynamics*, University of Michigan.

HENDERSON, R. D. & KARNIADAKIS, G. E. 1993. Unstructured spectral element methods for the incompressible Navier–Stokes equations. In *Proc. 8th Int. Conf. Finite Element Methods in Fluids*, Barcelona.

WILLIAMSON, C. H. K. & ROSHKO, A. 1988. Vortex formation in the wake of an oscillating cylinder. *J. Fluids & Struct.*, **2**, 355–381.